

Residual Properties of Gases Based on a Complete Virial Equation of State

L. Silberring¹

Received November 20, 1995

A particular virial equation of state is proposed for calculation of residual thermodynamic properties of real gases. It uses an infinite, nontruncated series of terms, but simplified, temperature-independent values of the virial coefficients are suggested beyond the third. Range limits of applicability are investigated along with their possible extensions. Within these range limits the suggested equation defines all residual thermodynamic properties of real gases and their mixtures, including partial molar residual properties of each component in the latter. Comparison with experimental evidence and with data calculated by other methods is discussed.

KEY WORDS: differential coefficients; real gases; residual properties; thermodynamic properties; virial coefficients.

1. INTRODUCTION

This paper treats residual properties of gases in such a range of parameters where adequate description of these properties by an analytical equation of state (EOS), explicit in pressure, is possible. Within the above range, this paper deals with all thermodynamic properties of gases. Suggestions are made for a derivation of transport properties from the information used to describe the thermodynamic properties. The results are compared with experimental evidence.

The subject reflects the results of continuing research, the initial concept of which was published in 1990 by the author [1]. The present text is, however, self-contained and does not require consultation of the

¹ Silberring Engineering Ltd., Wipkingerplatz 7, 8037 Zurich, Switzerland.

previous publication. The results of this work serve as one of the bases of a computer program system which is useful in determining properties of matter by a wide range of users.

Among a great number of the available EOS, the virial one (VEOS) is still the only one which defines not only the properties of pure gases, but also those of gas mixtures as soon as a minimum of additional experimental data on the latter is available. The particular form of the VEOS described in this paper covers a large, albeit still limited range of parameters. At subcritical temperatures this range is restricted to the vapor phase, including subcooled vapors, up to densities at which the isothermal pressure derivative with respect to the density remains positive. At supercritical temperatures the limits of the reduced (i.e., related to the critical value) density are between 0.6 and 2, depending on the temperature and desired accuracy.

Additive terms to the VEOS or any other EOS are necessary to extend the range of validity to the surroundings of the critical point of any pure gas or of the loci of critical parameters of any gas mixture. Recent advances in this field are discussed in Sections 5 and 9.

2. POSTULATES

The proposed VEOS is based on the available experimental evidence and on the following regularities deduced therefrom.

- (a) All virial coefficients $B(T)$, $C(T)$, $D(T)$, etc. (second, third, fourth, and so on), as well as all their temperature derivatives, each plotted as a function of temperature T , have a similar shape. In particular, their values approach negative infinity for even and positive infinity for odd derivatives, respectively, if the absolute temperature approaches zero. At the other end of the temperature scale, the virial coefficients approach a constant value, positive for the zeroth derivative and zero for all other derivatives. Between these two limits a single extreme value appears for each of the functions under consideration: a maximum or minimum for the even or odd derivatives, respectively. The position of any one of these extreme values moves toward decreasing temperatures with rising order of the derivative. All functions are monotonic on each side of the extreme value.
- (b) Within the already mentioned range of validity (which is further described in Section 3), virial coefficients of various number and

their temperature derivatives contribute quite differently to the residual properties of gases. It can, however, be observed that the absolute values of such contributions decrease with the rising number of the virial coefficient and, except between the zero and the extreme value of the ordinate, with rising temperature. Furthermore, it appears that the high-temperature asymptotic value of any n th virial coefficient is equal to a constant raised to the power $n - 1$. This constant depends only on the nature of gas. It is designated Y and called covolume throughout this work. Within the parameter range considered in this work, Y^{n-1} provides the sole relevant contribution of the virial coefficients, beyond the third, to the residual properties of gases.

The behavior of $B(T)$ has been observed experimentally for many gases and has been investigated within a wide range of temperatures. That of $C(T)$ is known within a narrower range of temperatures. Some associated examples are compared later in this paper with experimental evidence along with the effects of the postulated extensions beyond the latter.

3. THE COMPLETE LEIDEN-TYPE VEOS AND ITS COEFFICIENTS

Using the postulates described above, we can write the VEOS as follows:

$$Z = 1 + B\rho + C\rho^2 + \frac{(Y\rho)^3}{1 - Y\rho} \quad (1)$$

where ρ represents the density.

For any selected value of Y , Eq. (1) can be split into experimentally accessible terms and a linear function of ρ , namely,

$$\left[Z - 1 - \frac{(Y\rho)^3}{1 - Y\rho} \right] \frac{1}{\rho} = B + C\rho \quad (2)$$

The function $F(Y, \rho)$ on the left-hand side of the above equation can be used in a linear regression analysis to find the optimum values of B , C , and the associated correlation coefficient, everything as a function of Y . The optimum value of Y can be then selected as the one which coincides with the maximum value of the said correlation coefficient.

The above analysis must, however, be performed simultaneously with the selection of the previously described range limits, at least for some gases selected as relevant for the determination of such limits, presumed universal for all gases. The best experimental data for this purpose are those at temperatures above 1.5 times the critical temperatures and at densities up to twice the critical densities. Unfortunately, data in this parameter range are scarce and the available experimental information can be considered as adequate for a few gases only, e.g., He, H₂, D₂, Ar, N₂. The analysis described above has been performed for many gases beyond this list, but in many cases only a rough approximation of the optimum value of Y could be determined.

3.1. The Temperature Function for Virial Coefficients

Further regression analyses are necessary to find B and C as functions of temperature for each pure gas. First, a formula for these functions must be selected. It should be able to represent available experimental information within its tolerances while satisfying the criteria defined in Section 2. The following universal function for both $B(T)$ and $C(T)$ has been found by trial and error:

$$\frac{B(T)}{V_c^{n-1}} = \left(\frac{Y}{V_c}\right)^{n-1} + \sum_{q \rightarrow -\infty}^{\infty} A_{nq} e^{-K_{nq} T_r} \quad (3)$$

where $T_r = T/T_c$ is the reduced temperature, T_c and V_c are the critical temperature and volume (for quantum gases their classical values are defined by Gunn et al. [2]) of any pure gas, and $n=2$ and q are integers. The same formula remains valid when B and $n=2$ are replaced by C and $n=3$. The constants A_{n0} to A_{n3} and K_{n0} in the series on the right-hand side of the above equation are determined for each virial coefficient ($n=2$ and $n=3$) by a nonlinear regression analysis of the experimental information. The remaining constants are related to these five constants by the following formulae:

$$K_{nq} = 2^q K_{n0} \quad (4)$$

If $q < 0$ and $n=2$, then

$$A_{2q} = 0 \quad (5)$$

If $q < 0$ and $n=3$, then

$$A_{3q} = A_{30} (A_{32}/A_{31})^{q/2} \quad (6)$$

If $q > 0$, then the following relation holds for all A_{nq} :

$$\frac{A_{nq+3}/A_{nq+2}}{A_{nq+2}/A_{nq+1}} = \frac{A_{nq+2}/A_{nq+1}}{A_{nq+1}/A_{nq+0}} \quad (7)$$

If $q > 1$, then all constants A_{nq} are negative; otherwise, they are positive. All values of K_{nq} are positive. The two sets of five constants and the covolume Y , i.e., altogether 11 adjustable constants, describe all molar residual properties of each pure gas within the selected parameter limits.

The series on the right-hand side of Eq. (3) is rapidly converging in both directions around $q = 0$, with rising absolute value of q . It can, therefore, be truncated as soon as the contribution of the remaining terms becomes negligible. The number of relevant terms depends, however, on the gas, on the number of the virial coefficient and on the temperature.

The nonlinear regression has been performed for a number of gases, initially on B data calculated by the linear regression analysis of experimental data for each isotherm. Subsequently, C data from the linear regression analysis have been adjusted to deliver the estimated compression factor at each temperature near the range I (Table I) limit of density. Finally, the same kind of analysis as for the B data has been performed on the adjusted

Table I. Temperature-Dependent Density Limits for the Validity of Eq. (1)^a

Temperature range	Density range of molar residual properties	
	<i>I</i>	<i>II</i>
	Density limits, whichever is less for each temperature range	
$T \leq T_{yc}$	ρ_s ρ_{ys} $0.6\rho_c$	ρ_{ys} $0.9\rho^c$
$T_{yx} < T \leq T_c$ (if $T_c > T_{yc}$)	ρ_s $0.6\rho_c$	$0.9\rho_c$
$T \leq 1.5T_{cc}$	$0.6\rho_c$	$0.9\rho_c$
$1.5T_{cc} < T \leq 2T_{cc}$	$0.6\rho_c$	$2\rho_c$
$2T_{cc} < T$	$1.5\rho_c$	$2\rho_c$

^a c, critical point; yc, apparent critical point (defined in Section 5); ys, stability limit (defined in Section 5); s, saturated vapor density; cc, classical critical temperature of quantum gases (He, H₂, HD, D₂, Ne) and actual critical temperature of other gases.

values of C . Up to now the constants A_{nq} and K_{0q} have been estimated using the above method for 18 gases. For an additional 40 gases, most of them hydrocarbons, all necessary information has been prepared for a different method of calculation of B , C , and Y , described below.

3.2. Virial Coefficients from the Law of Corresponding States

Another procedure can deliver satisfactory results whenever specific experimental information is inadequate for the above-described analysis and whenever these gases are not strongly polar. In such cases the linear relation of Pitzer et al. [3–5] has been used together with information on two gases [indices 1 and 2 in Eq. (8)] with adequately different acentric factors to find not only B and Y but also C of a third gas [index 3 in Eq. (8)] as a function of its acentric factor ω_3 . This relation has been applied using the following equation:

$$\frac{B_{3,q \neq 0}(T_{r3}, \omega_3)}{V_{c3}^{n-1}} = \frac{\omega_2 - \omega_3}{\omega_2 - \omega_1} \frac{B_{1,q \neq 0}(T_{r1}, \omega_1)}{V_{c1}^{n-1}} + \frac{\omega_3 - \omega_1}{\omega_2 - \omega_1} \frac{B_{2,q \neq 0}(T_{r2}, \omega_2)}{V_{c2}^{n-1}} \quad (8)$$

where B , T_r , V_c , and ω designate, respectively, the second virial coefficient, the reduced temperature, the critical volume, and the acentric factor of the three gases, each of which bears the above-defined index. The additional index $q \neq 0$, associated with all values of B , indicates that the contribution of the term with index $q = 0$ shall be excluded from the sum on the right-hand side of Eq. (3) when B_1 and B_2 are calculated using this formula. For this particular term, the linear relation coefficients $(\omega_2 - \omega_3)/(\omega_2 - \omega_1)$ and $(\omega_3 - \omega_1)/(\omega_2 - \omega_1)$ of Eq. (8) shall be applied to the coefficients A_{n0} and K_{n0} instead of the value of the function generated by them; otherwise this function would not always fulfill postulate (a) of Section 2 at temperatures beyond the maxima of B or C .

Therefore if the critical parameters and acentric factors of all three gases are known and everything appearing on the right-hand side of Eq. (3) is known for the gases labeled 1 and 2, the $B(T)$ of the third gas can be found from Eq. (8). As in the case of Eq. (3), B and $n = 2$ can be replaced by C and $n = 3$. A fair validity of such an extension of the Pitzer's postulate has been confirmed by an appropriate inspection of the relevant properties of a variety of gases.

3.3. Temperature Derivatives of the Virial Coefficients and Their Graphical Representation

Not only the virial coefficients but also their temperature derivatives are needed for calculation of the various thermodynamic properties. The

nomenclature can be simplified if the derivatives of B and C , each multiplied by the appropriate power of the temperature, are designated as follows:

$$B' = TdB/dT \quad B'' = T^2dB/dT^2 \quad (9, 10)$$

$$C' = TdC/dT \quad C'' = T^2dC/dT^2 \quad (11, 12)$$

Analogous symbols are used for higher derivatives whenever they are needed, e.g., for the calculation of some differential coefficients.

Graphical representation of virial coefficients and their temperature derivatives as functions of temperature can be improved if a logarithmic temperature scale is used for the abscissa and the following operator $Q(X)$ is applied to the ordinate:

$$Q(X) = [\text{sgn}(X)][\ln(1 + |X|)] \quad (13)$$

where X stands for B or C or any of their temperature derivatives defined by Eqs. (9) to (12). For C , C' , and C'' it has been applied twice, consecutively.

The ratio of the covolume Y to the critical volume V_c of a number of gases investigated by the method described here has been found to be between 0.237 and 0.322. This can be compared with the low-volume (high-density) limits of validity of Eq. (1) at high temperatures, namely, between 0.5 (2) and 0.67 (1.5). These and other limits are summarized in Table I. Symbols appearing in this table and not encountered hitherto are explained in Section 5.

4. EXAMPLES OF VIRIAL COEFFICIENTS AND THEIR COMPARISONS WITH EXPERIMENTAL AND OTHER DATA

Two examples of the described method of estimation of the constants of Eq. (3) and the associated comparisons of the calculated PVT data with experimental or other data are discussed below. The data from various sources are shown by points, whereas solid or dashed lines represent the results of this work within ranges *I* and *II*, respectively. The abbreviated name of each source appears in the legend to each diagram. The figures were prepared using the values of the constants summarized in Table II.

4.1. Argon

The linear regression analyses of isotherms were performed using experimental data (MI) of Michels et al. [6, 7] and of Lecocq [8] for

Table II. Constants in Eqs. (7) and (13)

Symbol	Unit	Argon	Normal H ₂	Para-H ₂
Critical data (classical for hydrogen)				
T_c	K	150.66		43.6
V_c	cm ³ · mol ⁻¹	75.24		51.5
Other constants in Eq. (7)				
A_{20}	—	1.639 03 E-1		2.713 39 E-1
A_{21}	—	-8.500 97 E-2		-2.895 93 E-1
A_{22}	—	-1.401 32 E-1		-3.645 09 E-1
A_{23}	—	-2.643 61 E-1		-5.742 49 E-1
K_{20}	—	3.758 82 E-2		8.385 53 E-2
A_{30}	—	8.177 35		9.254 11 E-1
A_{31}	—	-6.448 45 E+5		-1.061 84 E+3
A_{32}	—	-5.532 69 E+6		-2.995 96 E+3
A_{33}	—	-4.920 13 E+7		-8.453 07 E+3
K_{30}	—	9.448 57		7.545 92
Y/V_c	—	0.302		0.258
Constants in Eq. (14) for the vapor-liquid equilibrium				
p_0	—	1.581 038	0.273 836 7	0.256 810 4
p_1	—	-4.763 781	-3.488 222	-3.589 047
p_2	—	-0.491 288 2	0.288 941 1	0.346 838 6
p_3	—	0	0	0
p_4	—	0.237 258 5	0.395 068 1	0.330 950 4

temperature ranges from 123.15 to 423.15 and from 573.15 to 1223.15 K, respectively. Unfortunately, Lecocq did not report his results at experimental densities but instead produced tables generated by his smoothing procedure. It is shown in Fig. I that these table values are not convenient for the method of analysis selected for this work. Therefore, only MI data from this figure were used for subsequent nonlinear regression analysis of the virial coefficients as a function of temperature. They have, however, been completed by data (LE) of Levelt Sengers et al. [9] at 80, 411.52, and 450 to 1300 K as well as by the data (PO) of Pope et al. [10], the only source of simultaneous experimental values of B and C at low temperatures.

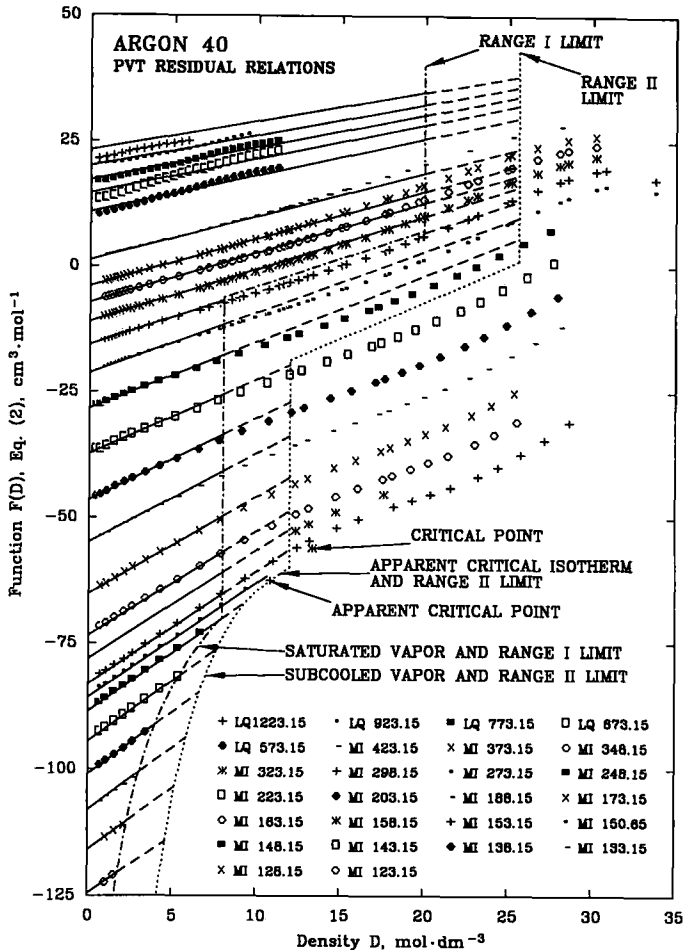


Fig. 1. *PVT* residual relations of argon. Comparison of experimental data with data of this work.

Figures 1 to 5 compare not only the said sets of *PVT* data, but also those (RB) of Robertson et al. [11] and those (SJ) of Stewart and Jacobson [12], with the results of this work. The importance of the selected range limits is evident from these diagrams. It is also shown in Fig. 5 that the SJ set of data implies a rather improbable sign and magnitude of *C* below 110 K.

Figures 6 and 7 compare, respectively, not only the second and third virial coefficients from the sources listed above but also those (GO) of

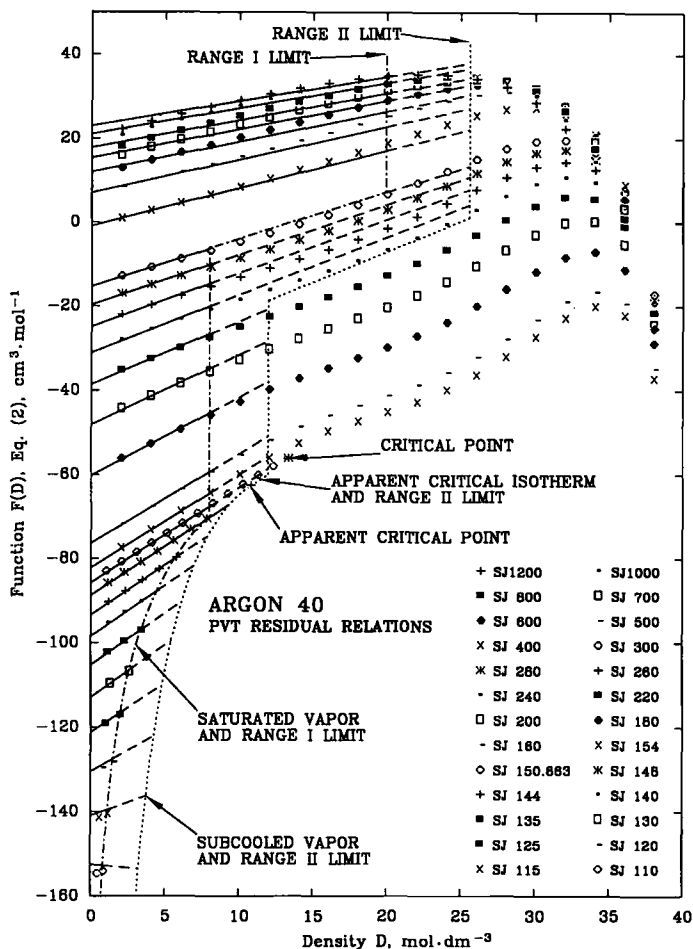


Fig. 2. PVT residual relations of argon. Comparison of data compiled by Stewart and Jacobsen [12] with data of this work.

Gosman et al. [13] and (KE) of Kestin et al. [14] with the values according to this work. The temperature derivatives of the virial coefficients are incorporated in these comparisons where they are available. It is shown in these figures that the agreement among the various sources and this work is reasonably good at least for B , B' , and B'' at supercritical temperatures. At lower temperatures the experimental evidence is scarce and the opinions of researchers diverge, especially in the case of C , C' and C'' . The consequences of this are discussed in Section 7.1.

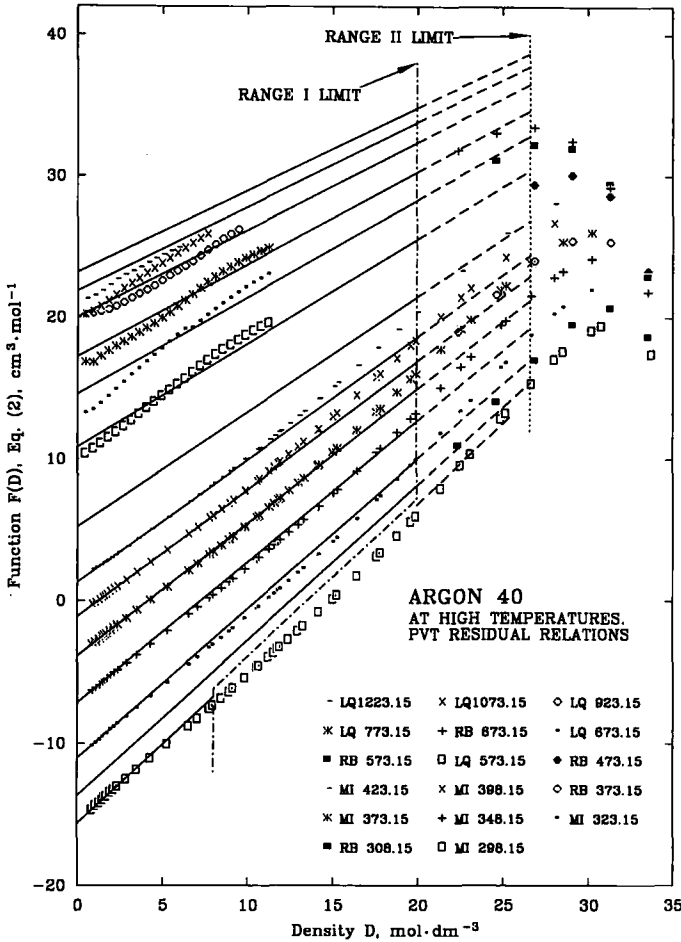


Fig. 3. *PVT* residual relations of argon at high temperatures. Comparison of experimental data with data of this work.

4.2. Hydrogen

Experimental *PVT* data (MI) of Michels et al. [15] are shown in Figs. 8 and 9 and have been used in this work within their range of temperature between 98.15 and 423.15 K. The results of their linear regression analysis used in this work as inputs to the subsequent nonlinear regression analysis of the virial coefficients as a function of temperature are not identical to the results derived from the same *PVT* data by Michels et al.

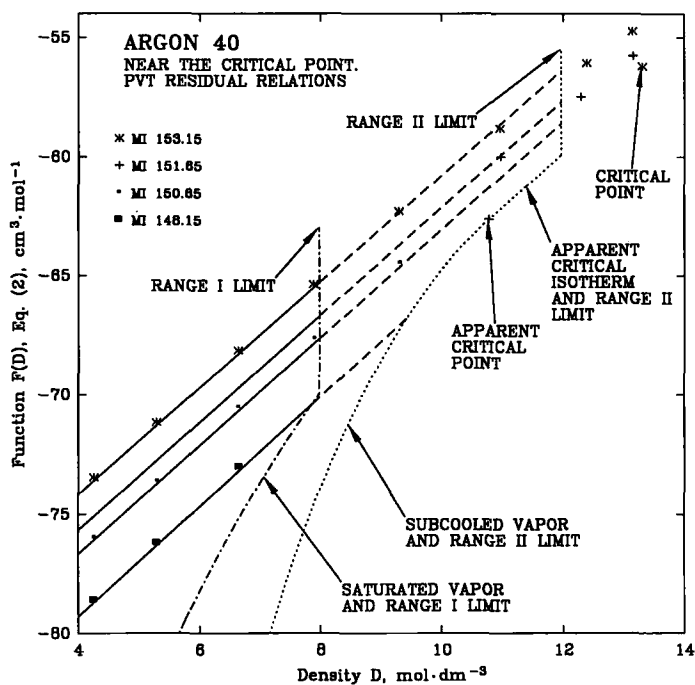


Fig. 4. PVT residual relations of argon near the critical point. Comparison of experimental data with data of this work.

[16] since both methods of analysis differ. The differences can be seen in Figs. 12 and 14 (enlarged version of Figs. 11 and 13), where the abbreviation MIP designates the values of the virial coefficients determined by Michels et al. using their method. Further (WSB) data of Woolley et al. [17] are shown in Figs. 8 and 10 for temperatures below the range of MI data.

At temperatures near the normal boiling point of normal hydrogen there are discrepancies among the estimations of the second virial coefficient. In particular, at a temperature of 20.4 K, the value of this coefficient has been found to be (in historical order) -145 , -152 , -150 , and $-145 \text{ cm}^3 \cdot \text{mol}^{-1}$, respectively, by Woolley et al. [17], Beenakker et al. [18], Knaap et al. [19], El Hadi et al. [20]. Knaap et al. did not find their value by direct experiments but used a slightly higher value than found by Beenakker et al. for their relative experiments in the temperature range between 20 and 70 K. Therefore, if their reference value is still too low then

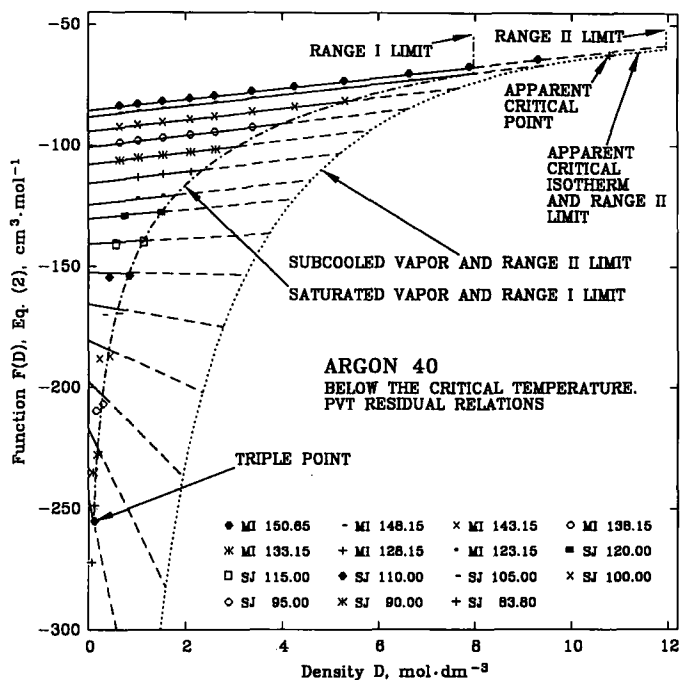


Fig. 5. *PVT* residual relations of argon. $T < T_c$. Comparison of experimental and other data with data of this work.

the values derived therefrom must also be revised. In this work the data (EH) of El Hadi et al. have been used as a basis of B in their experimental temperature range from 19.26 to 23.26 K. As a further input the datum (WSB) of Woolley et al. at 600 K has been used. The results of fitting are shown in Figs. 11 and 12. The data (MIP) of Michels et al. and (KN) of Knaap et al., as well as data (GOO) of Goodwin et al. [21] and (MC) of McCarty et al. [22], are also shown. The agreement between the data used as a basis and the results of this work is good. Significant differences with other data appear mainly in comparison of the temperature derivatives.

The aforementioned MI data were used as a main basis of the third virial coefficient. Below their temperature range and down to the critical temperature the input data for the fitting of C were derived from the WSB *PVT* data near the range I limit. Finally, the temperature at which C is zero was selected in agreement with MC data. The agreement between the values of C according to this work and the MI data is good, but not so

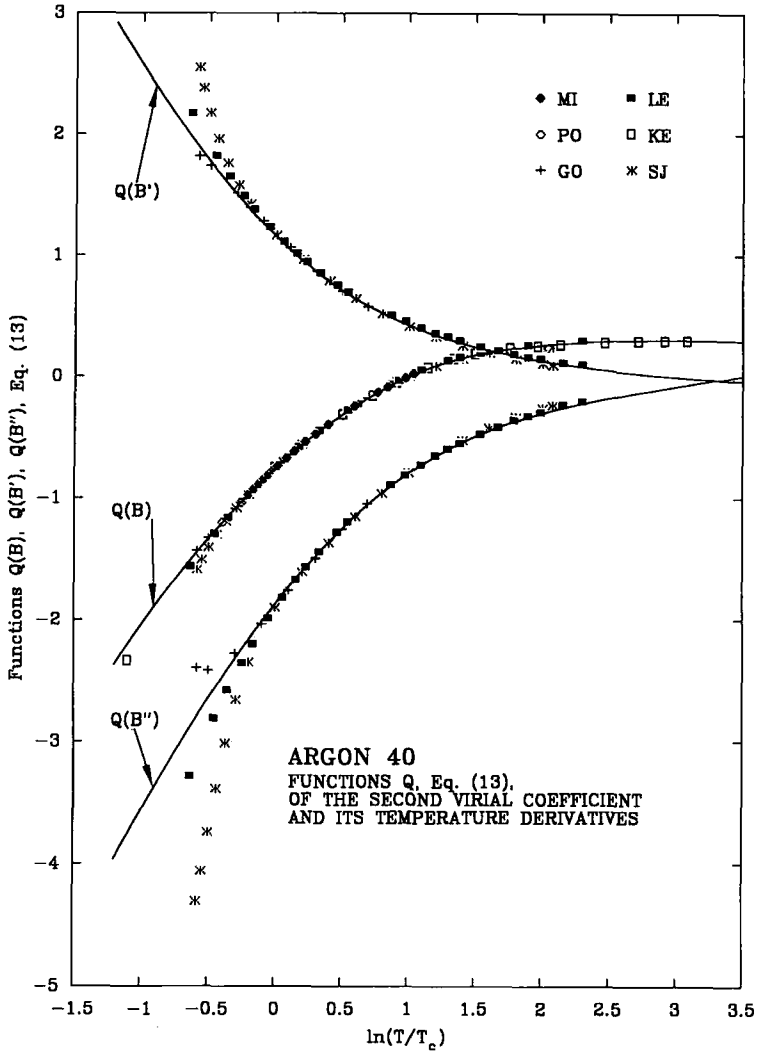


Fig. 6. Second virial coefficient of argon. Comparison of experimental and other data with data of this work.

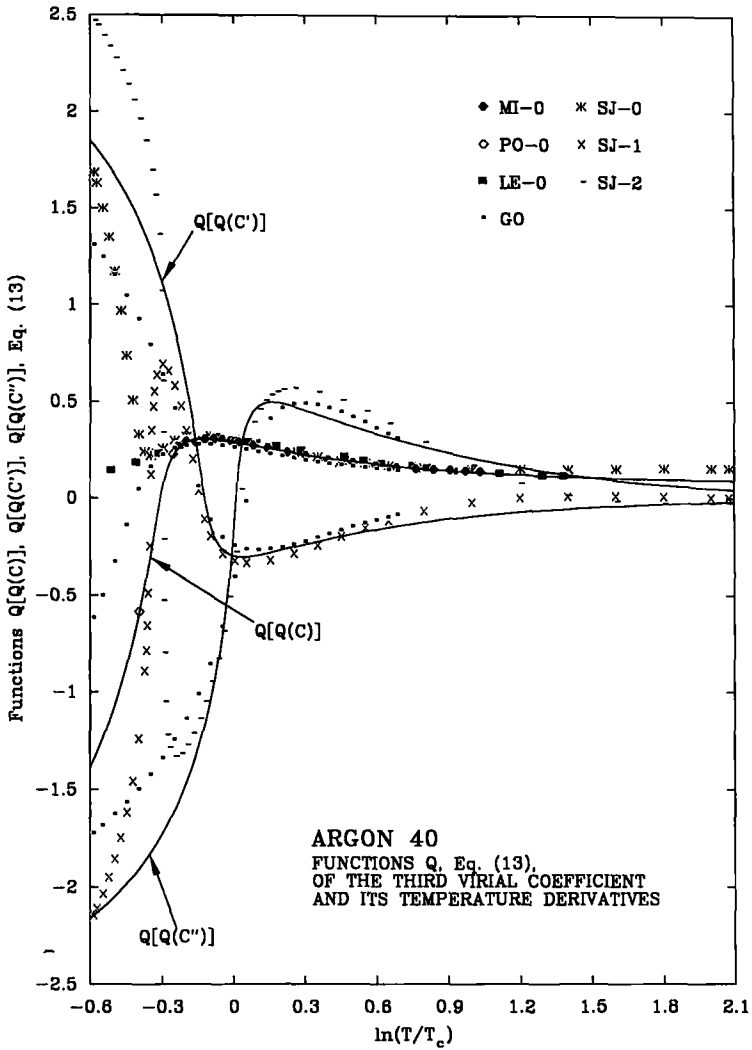


Fig. 7. Third virial coefficient of argon. Comparison of experimental and other data with data of this work.

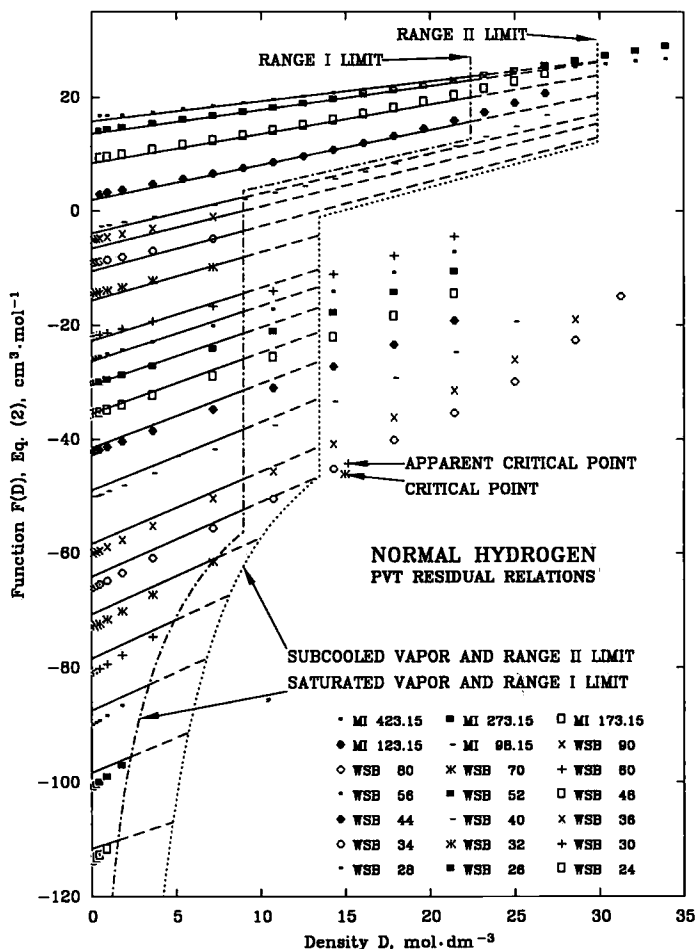


Fig. 8. PVT residual relations of hydrogen. Comparison of experimental and other data with data of this work.

with other sources at low temperatures. In particular, C' and C'' near the (classical) critical temperature are quite different from GOO and MC data (these two data sets are similar below, and identical above, 100 K). Unfortunately, as mentioned in the MC paper, the tolerances of these data are inadequately known. Further adjustments may be made as soon as more experimental information is available.

Measurements of Beenakker et al. [23] show that even at quite low temperatures (18.3 and 20.5 K), the differences between the second virial

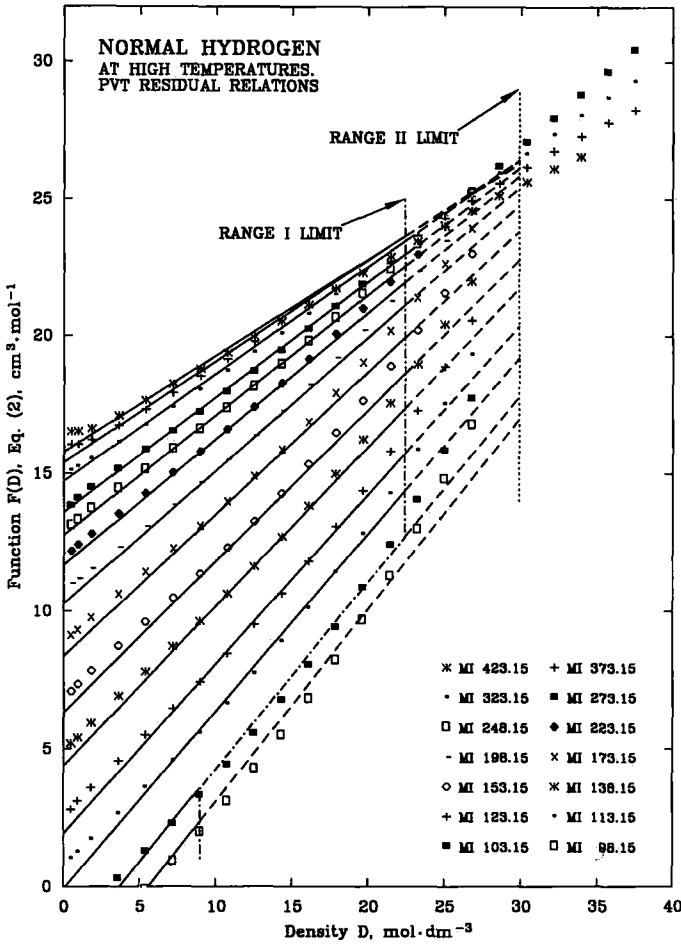


Fig. 9. PVT residual relations of hydrogen at high temperatures. Comparison of experimental data with data of this work.

coefficient of para and normal hydrogen do not exceed the tolerances of the experimental results. It may, therefore, be concluded (as did McCarty et al. [22]) that any difference between the molar residual properties of ortho and para hydrogen is below the tolerances of the available information. The vapor pressures of para and normal hydrogen are, however, significantly different, and perfect-gas properties at low temperatures are very different.

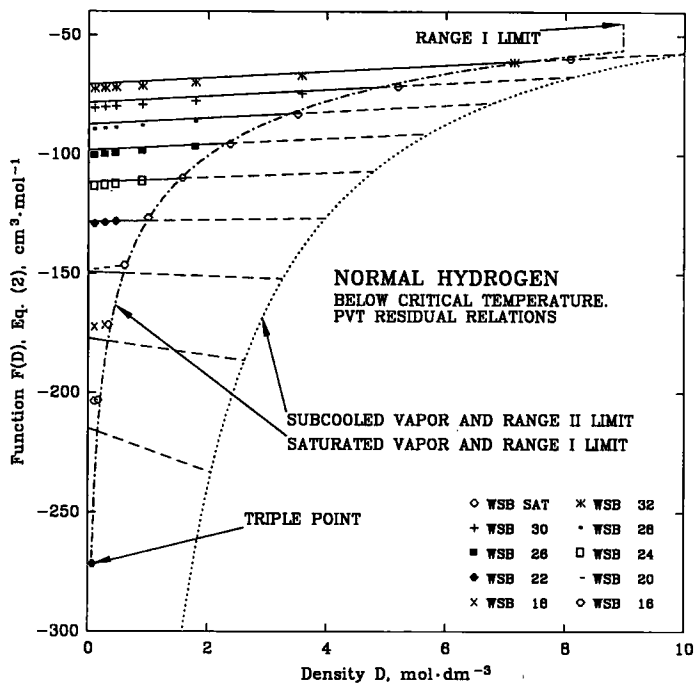


Fig. 10. *PVT* residual relations of hydrogen below the critical temperature. Comparison of experimental and other data with data of this work.

4.3. The Saturated Vapor Pressure Function in the Examples

The following universal function has been developed by the author for the saturated vapor pressure as a function of temperature:

$$\ln(P/P^\circ) = p_0 + p_1\vartheta + (p_2\vartheta^2/2) + (p_3\vartheta^3/6) + p_4E(\vartheta) \quad (14)$$

where P° is any reference value of pressure, e.g., its unit, $\vartheta = T/T_c - 1$, p_0 to p_4 are adjustable constants, and

$$E(\vartheta) = \iint (e^{-\vartheta}/\vartheta) d\vartheta d\vartheta \quad (15)$$

Two of the five adjustable constants of Eq. (14), namely, p_0 and p_1 , are simultaneously the integration constants of Eq. (15). A description of the

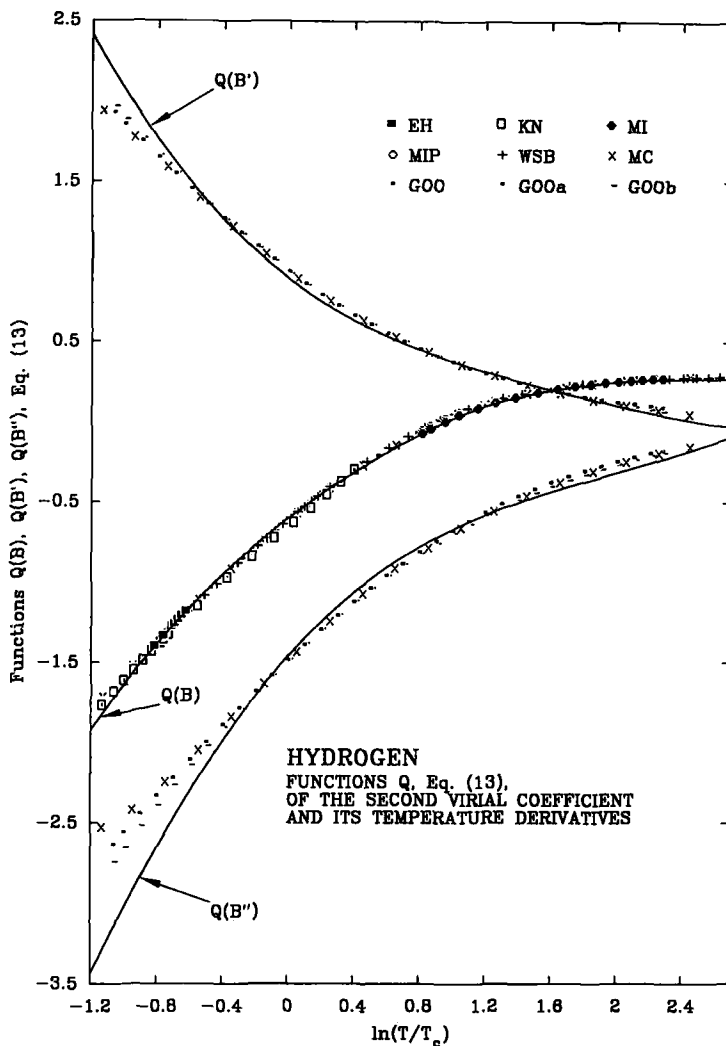


Fig. 11. Second virial coefficient of hydrogen. Comparison of experimental and other data with data of this work.

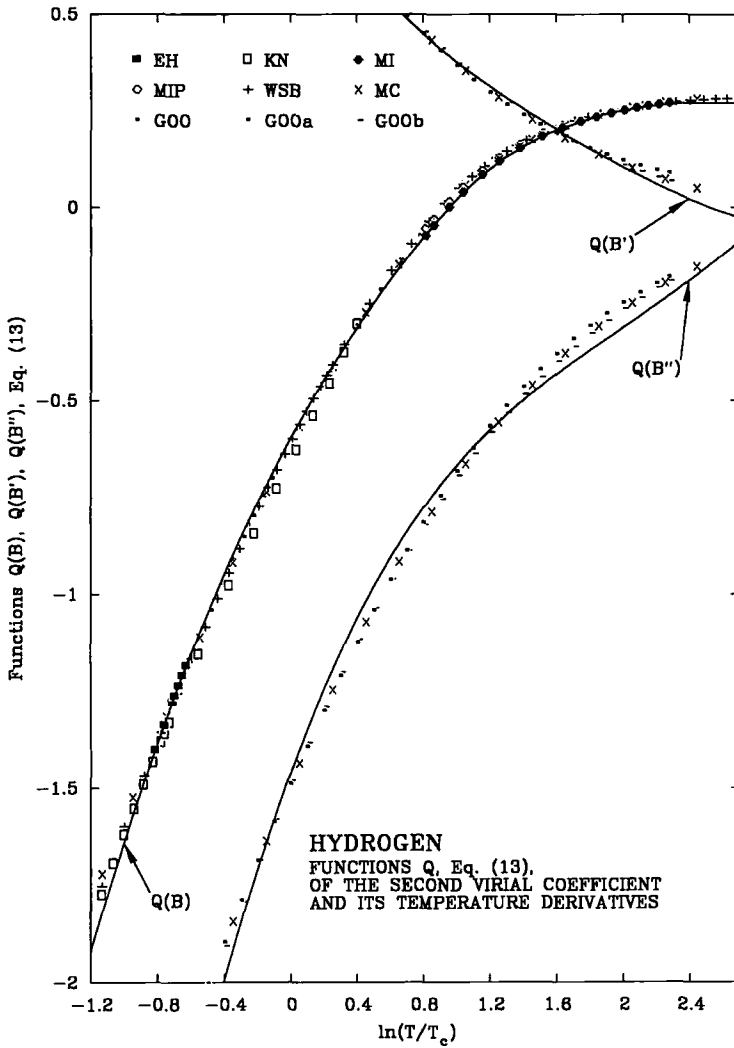


Fig. 12. A portion of Fig. 11 on an enlarged scale.

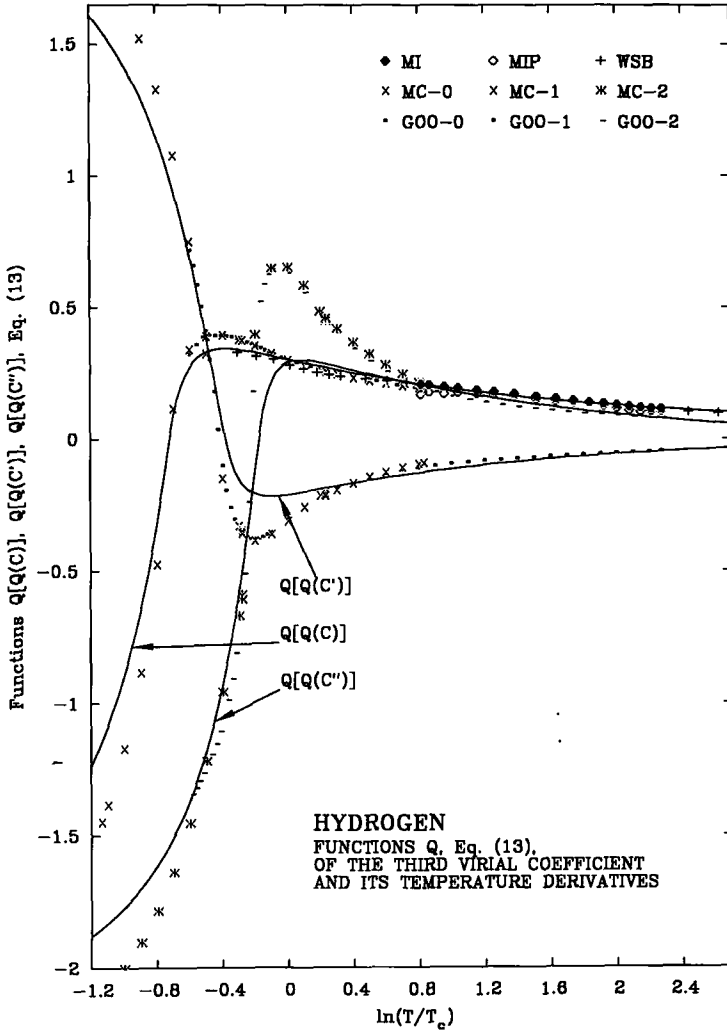


Fig. 13. Third virial coefficient of hydrogen. Comparison of experimental and other data with data of this work.

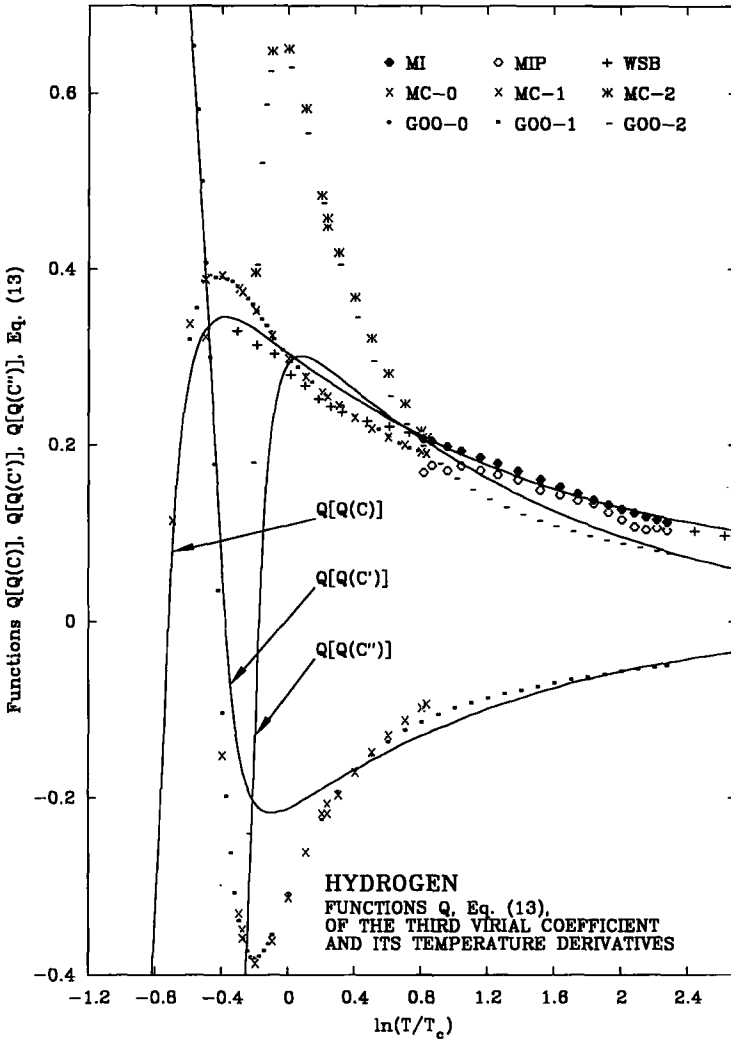


Fig. 14. A portion of Fig. 13 on an enlarged scale.

development of Eqs. (14) and (15) and a discussion of their particularities are beyond the scope of this paper. The values of the adjustable constants for Ar, para-H₂, and normal H₂ are, however, listed in Table II, whereby it should be noted that for the latter case Eq. (14) delivers the bubble-point pressure of a liquid with normal mole fractions of para-H₂ and ortho-H₂.

Equation (14) is valid at least within the same range of saturated vapor densities as specified in Table I for the whole-gas phase. The results of its application appear in some of the diagrams discussed in this section as well as in Section 7.

5. SOME PARTICULAR PROPERTIES OF THE PROPOSED VEOS

The high-temperature limit of the compression factor Z calculated by Eq. (1) can be represented by the following simple formula, in which B and C are replaced by their corresponding limits:

$$\lim_{T \rightarrow \infty} Z = \frac{1}{1 - Y\rho} \quad (16)$$

The above equation is identical to that of van der Waals and some other cubic EOS if their terms associated with the attractive intermolecular forces are omitted. The temperature-independent constant Y is identical with the covolume appearing in cubic EOSs.

One conclusion from Eqs. (1) and (16) could be that ρ has an upper limit [$\rho < (1/Y)$], but none of these equations is valid up to this limit as may be seen, e.g., from Figs. 2 and 3. A better conclusion is, therefore, that the covolume in the VEOS considered here appears as a constant only as far as it is not approached too closely. Beyond such approach the VEOS (1) becomes invalid since ρ can rise significantly beyond $1/Y$, while both the compression factor and the pressure remain finite. At some moderately high pressure, the hitherto apparently rigid covolume yields and the further rise of the pressure is significantly reduced until the volume reaches a value well below Y . Some of the associated research has been described by Ross and Young [24].

Equation (1) defines the compression factor Z in terms of a third degree polynomial and the pressure $P = ZRT\rho$ in terms of a fourth-degree polynomial in density ρ . The latter has only one root at which $0 < \rho < (1/Y)$, $P > 0$, $(\partial P/\partial \rho)_T = 0$, and $(\partial^2 P/\partial \rho^2)_T = 0$. The above conditions are designated by indices yc , and the associated parameters are called apparent critical point parameters below. They are not very different from experimental critical conditions but they cannot be forced to coincide with the latter by modifying the coefficients on the right-hand side of Eq. (1). In particular, it can be shown that the lowest value of Z_{yc} is $1/3$ (if $Y=0$), and this is higher than the maximum observed value of the critical compression factors Z_c .

All density limits retained for the validity of the suggested VEOS within the mentioned density ranges *I* and *II* are specified in Table I.

Below the apparent critical temperature T_{yc} a locus of densities $\rho_{ys}(T)$ can be found, so that $0 < \rho_{ys} < \rho_{yc}$, $P_{ys}(\rho_{ys}, T) < P_{yc}$, $(\partial P_{ys}/\partial \rho)_T = 0$, and $(\partial^2 P_{ys}/\partial \rho^2) < 0$. This is the locus of maximum stable densities which can be represented by Eq. (1) below the apparent critical temperature. It is called the stability limit below [more precisely: absolute stability limit beyond which $(\partial P/\partial \rho)_T < 0$ within a parameter range, most of which is usually occupied by a metastable subcooled vapor]. The densities ρ_{ys} , calculated by the VEOS (1), are usually, but not always, higher than the saturated vapor densities. The stability limit then coincides with the metastable subcooled vapor limit, which has been simultaneously selected as the range II limit for temperatures below T_{yc} and for densities below 0.9 of the critical density. The scarce experimental data on subcooled vapors are in fair agreement with the data extrapolated using Eq. (1) within the limit described above.

The stability limit, calculated using the VEOS (1), can cross the saturated vapor line near the critical point and may even do so below the fraction of the critical density selected as the range I limit for the saturated vapor. In such cases Eq. (1) cannot describe the saturated vapor properties at densities exceeding the value at the crossing point. Both range limits may coincide between the crossing point and the maximum density selected for the range I limit if the latter exceeds the density at the crossing point. In examples illustrated in Figs. 1, 2, 4, and 5, this is not yet the case. It would become so if the dotted line crossed the dashed-dotted line to the left of the range I limit.

If the density exceeds the stability limit, described above, $(\partial P_s/\partial \rho)_T$ becomes negative, and at least the initial part of the associated range becomes inaccessible for experiments. The suggested VEOS does not attempt to describe anything beyond this limit, e.g., to define the properties of saturated or compressed condensed phase(s). Section 9 includes some further discussion of the associated questions.

6. MOLAR RESIDUAL THERMODYNAMIC PROPERTIES

Any real-gas property can be split into two additive terms namely, the perfect and residual terms. The former, usually much better known than the latter, are defined for the purpose of this work at any set of parameters as properties of such a hypothetical gas which would remain perfect when either its density or its pressure rises isothermally from a low value to the actual value. The selection of this low value is such that all deviations of a real gas from a perfect one become negligible. This definition, similar but not identical to the usual standard state definition, serves as a tool for

a sharp comparison of results, calculated by the suggested VEOS, with experimental data or with data based on other EOSs. It includes the perfect-gas contribution of the real-gas density or pressure in the perfect-gas entropy. This contribution is independent of EOS and, therefore, could blur the relevant magnitude of relative differences among the residual thermodynamic properties calculated by different methods or between any such sets of data and the experimental evidence.

As already mentioned, all molar residual properties can be calculated using the universal functions written in the previous sections and only 11 adjustable constants for each pure gas. The above number is reduced to one single constant, namely, the acentric factor ω , if the calculation is performed using Eq. (8).

The properties of a perfect gas, defined at the same density as the real gas (for an isochoric comparison with the properties of the latter), are different from those which are defined at the same pressure (for an isobaric comparison). The residual properties must, therefore, also depend on the above selection since the sum of both terms must be identical in both cases. In the comparisons discussed later the isochoric comparisons are used whenever experimental or other values of internal energy, internal free energy (Helmholtz function), entropy, or isochoric heat capacity are known as functions of density (or volume). Accordingly, the isobaric comparisons are used whenever such values of enthalpy, free enthalpy (Gibbs function), entropy, or isobaric heat capacity are known as functions of pressure.

Pressure and density are interrelated by Eq. (1); either can, therefore, be found if the other is known within the selected range II limits, except if the density sought coincides precisely with the stability limit. Any of the sets of the thermodynamic properties listed above is also related to the other set by well-known formulae. The explicit formulae for calculation of the molar residual properties have been derived using this basis and the well-known relations of thermodynamics. They are available to interested readers upon request.

7. EXAMPLES OF MOLAR RESIDUAL THERMODYNAMIC PROPERTIES AND THEIR COMPARISONS WITH EXPERIMENTAL AND OTHER DATA

A number of experimental values of molar residual properties of gases has been compared with data calculated by the formulae in this work. A few examples are described below. As in the case of the PVT data, values of the molar residual properties according to this work are shown in

diagrams by solid and dashed lines within the previously defined ranges *I* and *II*, respectively, whereas experimental data from other compilations are represented by points.

7.1. Argon

Molar residual isochoric heat capacity, internal energy, and entropy originating from compilations of Angus et al. (AN) [25] and of Stewart

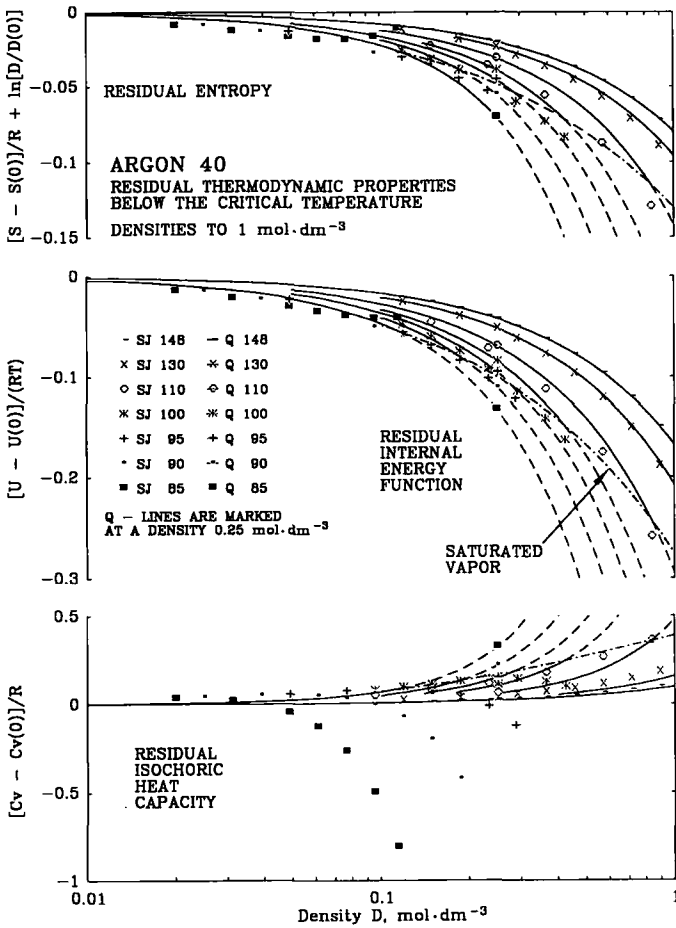


Fig. 15. Residual thermodynamic properties of argon. $T < T_c$; $\rho < 1$ mol·dm⁻³. Comparison of data compiled by Stewart and Jacobsen [12] with data of this work.

and Jacobsen (SJ) [12] have been compared with data (Q) from this work in Figs. 15 to 17. The agreement is fair, except for the most important values, namely, those of the molar residual isochoric heat capacity.

At temperatures below 110 K the available experimental information is inadequate to deduce therefrom the values sought. Hence all data shown are extrapolated. It is, however, unlikely that the molar residual isochoric

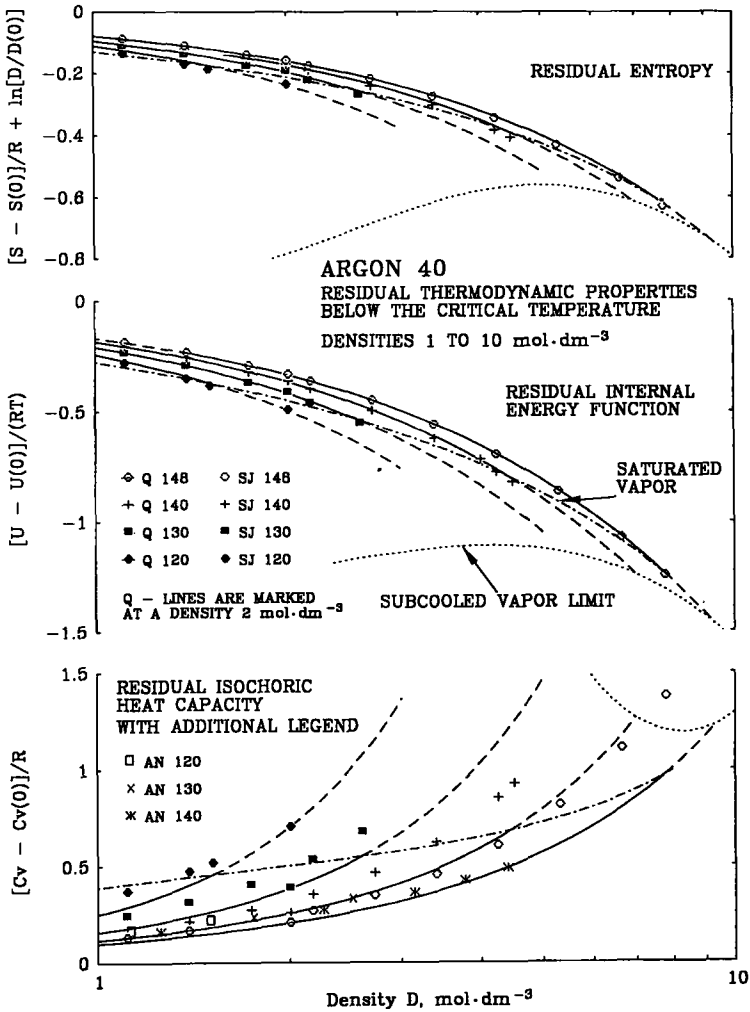


Fig. 16. Residual thermodynamic properties of argon. $T < T_c$; $1 < \rho < 10$ mol·dm⁻³. Comparison of data compiled by others with data of this work.

heat capacities assume negative values in this temperature range, as follows from the SJ formulations. Such results are rather a consequence of the improbable excursions of the extrapolated temperature derivatives of the third virial coefficient shown in Fig. 7. The authors have detected the problem and have excluded the associated data from their tables. They remain, however, implied in the tabulated values of the internal energy,

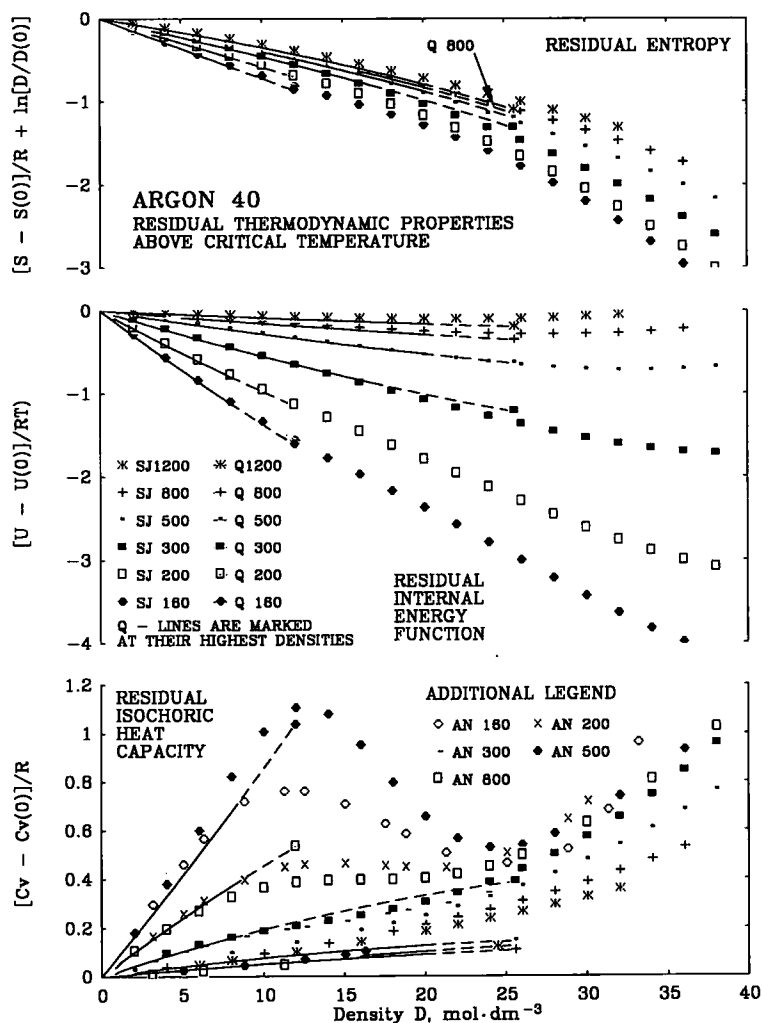


Fig. 17. Residual thermodynamic properties of argon. $T > T_c$. Comparison of data compiled by others with data of this work.

enthalpy, and entropy. AN data, deduced from but not fully identical to data of Gosman et al. [13], specify molar residual heat capacities near zero in this temperature range, and this is in agreement with the results of this work.

At higher temperatures most data in this work are situated between the AN and SJ values.

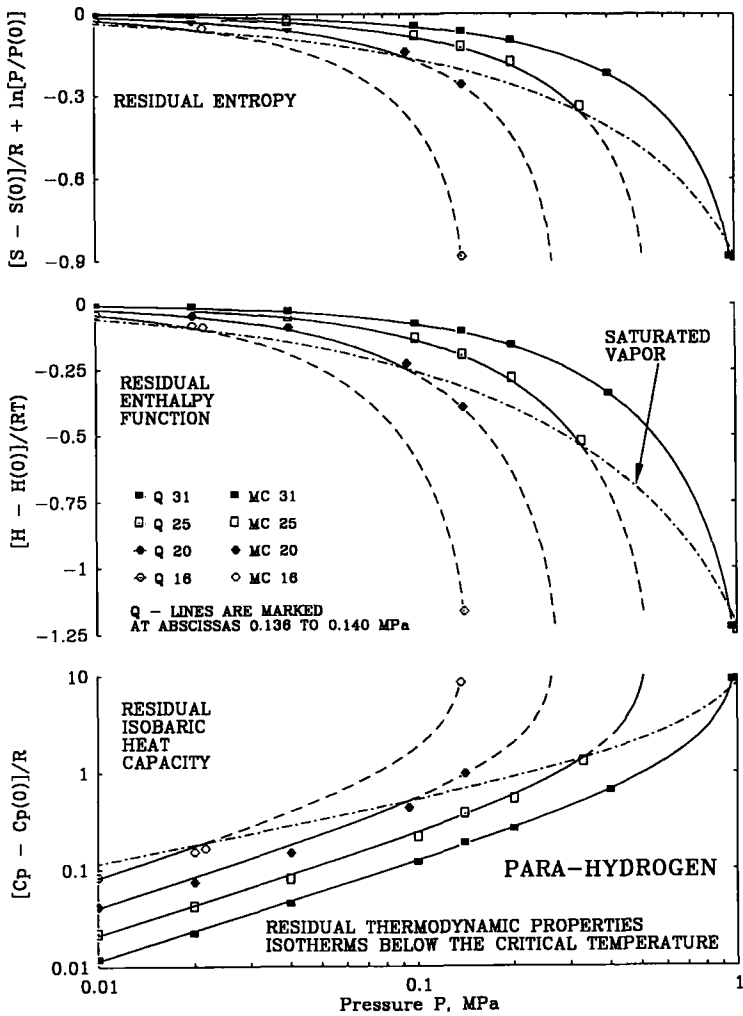


Fig. 18. Residual thermodynamic properties of hydrogen. $T < T_c$. Comparison of data compiled by McCarty et al. [22] with data of this work.

7.2. Hydrogen

Hydrogen properties have been extensively investigated, and accordingly, a better precision of well compiled molar residual properties than in the case of many other gases can be expected. In this case the molar residual isobaric heat capacity, enthalpy, and entropy have been plotted as

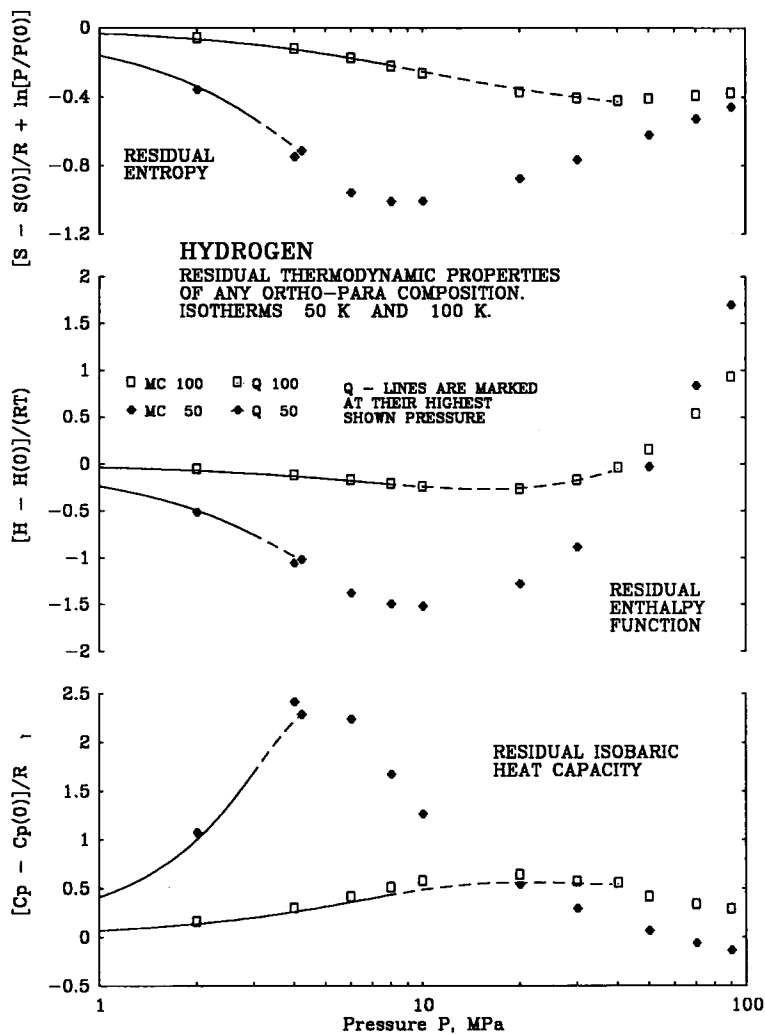


Fig. 19. Residual thermodynamic properties of hydrogen at 50 and 100 K. Comparison of data compiled by McCarty et al. [22] with data of this work.

functions of pressure in Figs. 18 to 20 to compare them with data (MC) of McCarty et al. [22], specified in their tables also along isobars.

The differences between the MC values of the temperature derivatives of the third virial coefficient and the corresponding values of this work near the classical critical temperature (Fig. 13) did not significantly affect the

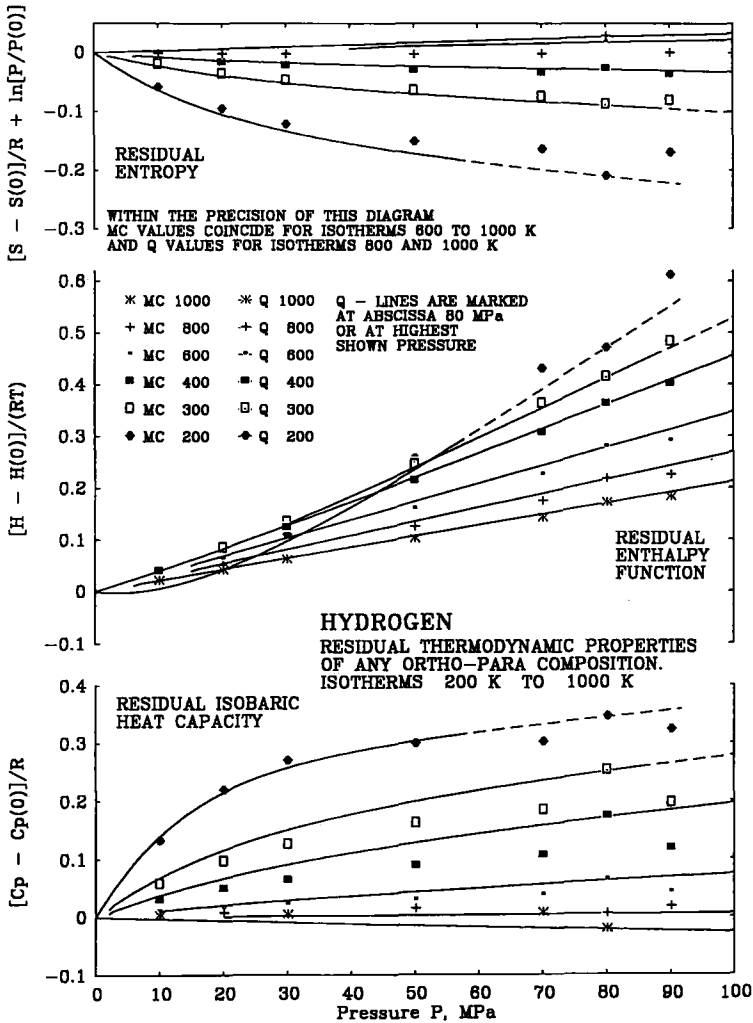


Fig. 20. Residual thermodynamic properties of hydrogen. $200 \leq T \leq 1000$ K. Comparison of data compiled by McCarty et al. [22] with data of this work.

good agreement of molar residual isobaric heat capacity in both sets of data. In fact, the sign of both differences is opposite and their absolute values are nearly inversely proportional to their contributions to the relevant function, so it remains difficult to find out which values of virial coefficients are nearer the truth.

At high temperatures and pressures the differences between both compared sets of data are significant. The smoothness of isochores (not shown) according to this work seems better than for MC data, but in any case, more and more reliable experimental information is necessary to improve the precision of molar residual properties in this range.

8. DIFFERENTIAL COEFFICIENTS

A number of other thermodynamic properties of any pure gas or any mixture of them, in particular various differential coefficients, sound velocity, etc., can be calculated on the basis of equations given in the previous sections. Some such coefficients are useful in fluid dynamics and have been defined, among others, by Eichelberg [26], Dzung [27, 28], Flatt [29, 30], and Flatt and Trichet [31]. The associated explicit formulae, which follow as far as applicable the definitions and the notation in the above references, are available to readers upon request.

9. OUTLOOK

The author's intention is to continue the extension of the coverage of properties of matter by his work initiated in the 1980s.

The already mentioned next step, namely, the extension to mixtures has been prepared and may appear soon. A further step is well advanced and may also be published in a separate paper. It consists of an extension to properties of the saturated condensed phase(s), liquid or solid, below the critical temperature. For this purpose and for pure substances it is necessary and adequate to use two additional functions, namely, the saturated vapor pressure $P(T)$, mentioned in Section 4, and the density $\rho_s(T)$ or volume $V_s(T)$ of the saturated condensed phase(s), each as a function of temperature. Both these functions are well accessible for experiments and ample experimental information is available on many substances over a wide temperature range. A variety of equations has been proposed for them; a universal function $P(T)$, introduced in Section 4.3 without details of its development, will be described elsewhere by the author. All thermodynamic properties of the condensed phase(s), of pure

substances, each in equilibrium with its vapor can be calculated using the above information and the general relations of thermodynamics, in particular, the Clausius–Clapeyron equation.

For further extension to the ranges of compressed condensed phases, an EOS for the latter is necessary. The pressure explicit form of VEOS is not suitable for this objective, and at least below the critical temperature, the necessary EOS need not be of the same type as the one selected for the gas phase.

The agreement between the experimental data at high temperatures and densities and data calculated using a VEOS similar to Eq. (1) could be improved by using a temperature-dependent fourth and possibly even higher virial coefficients instead of the powers of the temperature-independent covolume. The available experimental information under the said conditions is, however, inadequate for selection of an appropriate universal function and for determination of its coefficients. Such improvements must, therefore, wait for additional experimental data.

As already mentioned, the coverage of the present work, including its above described easy extensions, still leaves an important gap in the parameter space of interest. This gap starts at a subcritical temperature above which neither VEOS (1) is good enough for the properties of the saturated vapor nor is any other analytical EOS satisfactory for the properties of any phase. When the temperature rises to about 1.5 to 2 times the critical value, the gap ends and VEOS (1) with its possible improvements can again deliver satisfactory data. Between the above temperature limits the applications of VEOS must remain below the critical densities.

The said limits of the parameter space cannot be significantly extended by modification of, or by complements to, VEOS without violation of one of the postulates listed in Section 2. As already mentioned, even if these postulates were abandoned, it remains impossible or at least difficult to describe correctly the properties of gases over a significant range of temperatures and densities around the critical point by VEOS or by any other analytical EOS.

For many years the traditional development of various EOS has been governed by a tendency to approach the critical point as closely as possible. This has been achieved by a number of complements and modifications to the original form of the VEOS. In this process, the proposed forms of EOSs became complex. More importantly, the ability to deduce the properties of mixtures and the partial molar properties of their components from the properties of pure gases has been lost or, at least, impeded. The associated disadvantages became evident not only near the critical point, but also in the parameter space in which the original VEOS would be good enough.

Nonanalytical parametric functions have been developed for the surroundings of the critical point of some pure fluids, e.g., by Vicentini-Missoni et al. [32] for CO₂, Xe, and ⁴He, by Levelt Sengers et al. [33] for ³He, ⁴He, Xe, CO₂, O₂, and H₂O, by Angus et al. [34] for CO₂, and by Kestin et al. [35] for H₂O. A review of the associated research has been published by J. V. Sengers et al. [36]. A narrow range of the critical region has been traditionally selected, with the aim of completing some of the earlier, usually quite complex, analytical EOSs for the same gas.

The nonanalytical parametric functions can cover the entire gap of the parameter space described above. In such a case the abilities of the original VEOS for gas mixtures can be conserved, at least in the remaining parameter space, restricted as specified in Table I. Furthermore, it would be very useful if at least some conclusions for gas mixtures could be deduced from the parametric functions valid for pure fluids. Recent research in this area, reported by Sengers et al. [37–40], looks promising for this purpose.

As mentioned in Section 5, additional complements to the VEOS are mandatory to make it valid for the properties of fluids at densities exceeding 1.5 to 2 times the critical density.

The experimental basis of the second virial coefficient expressed by Eq. (3) can be widened. This equation is useful for calculation of not only the zeroth but also any subsequent temperature derivative of the virial coefficients. From all of the latter, the intermolecular potential of forces between the pairs of molecules can be found by inverse Laplace transformation as pointed out by Mason and Spurling [41]. Subsequently, transport properties at moderate densities can be calculated therefrom and compared with experimental data. Afterward, the form and the coefficients of the Eq. (3) can be improved as deemed necessary.

Some considerations may be useful with a view to improving the experimental basis for the scrutiny of properties of fluids. Most of the available experimental data on residual properties of gases is centered on the *PVT* relationship. This has certainly been inspired by simple access of such data for experimentation and by James Clerk Maxwell, who has shown that everything else can be found therefrom by differentiations. The latter would be easy to perform if the available experimental information could be fitted into reliable and sufficiently precise analytical functions. But this is not the case, and consequently, important losses of precision occur when residual thermodynamic properties are derived from experimental *PVT* data, even if the precision of the latter is high.

The other way round may lead to better results. Such molar residual properties as isobaric or even isochoric heat capacities, the Joule–Thomson coefficient, the speed of sound, and the like are experimentally accessible

and have already been used to some extent for scrutiny of all properties, including the testing of experimental *PVT* data. The mathematical operations necessary for this route may be more complex than for the usual methods. It would be necessary to solve sets of partial differential equations, sometimes by numeric methods, and the associated integration constants must also be found somehow. If all the pros and cons of both ways are considered, then the present, rather poor knowledge of such properties as, e.g., the residual heat capacities, could probably be improved by switching the focus of experimentation rather than by attempting to raise the precision of the prevailing methods of experiments. Probably better *PVT* data might also be achieved as a by-product of such switching.

ACKNOWLEDGMENTS

The author is indebted to a number of persons for valuable information and advice related to the subject and received from them personally or by correspondence over a number of years. Among them he is especially indebted to Professor H. H. Günthard at the Swiss Federal Institute of Technology in Zürich, to the late Professors J. Kestin and E. A. Mason at Brown University in Providence, R.I., to Professor W. A. Wakeham of the Imperial College in London, and to Mr. R. Flatt at the Swiss Federal Institute of Technology in Lausanne. Mr. J. C. Trichet at the École Polytechnique Féminine, Sceaux, France, and Mr. R. Flatt kindly inspected the manuscript and suggested some modifications and corrections, which have been incorporated as far as possible.

REFERENCES

1. L. Silberring, in *Data for Discovery, Proc. 12th Int. CODATA Conf., July 15-19, 1990 Columbus, OH, U.S.A.*, Ph. S. Glaeser, ed. (Begell House, New York, 1992), p. 366.
2. R. D. Gunn, P. L. Chueh, and J. M. Prausnitz, *AIChE J.* **12**:937 (1966).
3. K. S. Pitzer, *J. Am. Chem. Soc.* **77**:3427 (1955).
4. K. S. Pitzer, D. Z. Lippmann, R. F. Curl, Jr., C. H. Huggins, and D. E. Petersen, *J. Am. Chem. Soc.* **77**:3433 (1955).
5. K. S. Pitzer and R. F. Curl, Jr., *J. Am. Chem. Soc.* **79**:2369 (1957).
6. A. Michels, Hub. Wijker, and Hk. Wijker, *Physica* **15**:627 (1949).
7. A. Michels, J. M. Levelt, and W. De Graaff, *Physica* **24**:659 (1958).
8. A. Lecocq, *J. Rech. CNRS* **50**:55 (1960).
9. J. M. H. Levelt Sengers, M. Klein, and J. S. Gallagher, in *AIP-Handbook* (McGraw-Hill, New York, 1972), pp. 4-204.
10. G. A. Pope, P. S. Chapple, and R. Kobayashi, *J. Chem. Phys.* **59**:423 (1973).
11. S. L. Robertson, S. E. Babb, Jr., and G. J. Scott, *J. Chem. Phys.* **50**:2160 (1969).
12. R. B. Stewart and R. T. Jacobsen, *J. Phys. Chem. Ref. Data* **18**:639 (1989).
13. A. I. Gosman, R. D. McCarty, and J. G. Hust, *NSRDS-NBS* **27** (1969).

14. J. Kestin, K. Knierim, E. A. Mason, B. Najafi, S. T. Ro, and M. Waldman, *J. Phys. Chem. Ref. Data* **13**:229 (1984).
15. A. Michels, W. De Graaff, T. Wassenaar, J. M. H. Levelt, and P. Louwerse, *Physica* **25**:25 (1959).
16. A. Michels, W. De Graaff, and C. A. Ten Seldam, *Physica* **26**:393 (1960).
17. H. W. Woolley, R. B. Scott, and F. G. Brickwedde, *NBS* **41**:RP1932 (1948).
18. J. J. M. Beenakker, F. H. Varekamp, and A. Van Itterbeek, *Physica* **25**:9 (1959).
19. H. F. P. Knaap, M. Knoester, C. M. Knobler, and J. J. M. Beenakker, *Physica* **28**:21 (1962).
20. Z. E. H. A. El Hadi, J. A. Dorrepaal, and M. Durieux, *Physica* **41**:320 (1969).
21. R. D. Goodwin, D. E. Diller, H. M. Roder, and L. A. Weber, *J. Res. NBS* **68A**:121 (1964).
22. R. D. McCarty, J. Hord, and H. M. Roder, *Selected Properties of Hydrogen*, NBS MN 168 (1981).
23. J. J. M. Beenakker, F. H. Varekamp, and H. F. P. Knaap, *Physica* **26**:43 (1960).
24. M. Ross and D. A. Young, *Annu. Rev. Phys. Chem.* **44**:61 (1993).
25. S. Angus and B. Armstrong, *International Thermodynamic Tables of Fluid State*. Argon (Butterworths, London 1972).
26. G. Eichelberg, *Forschungsarbeiten Ing. Wes.*, Heft 220 (Berlin, 1920).
27. L. S. Dzung, *Schweiz. Arch.* **10**:305 (1944).
28. L. S. Dzung, *Z. angew. Math. Phys. (ZAMP)* **6**(14):207 (1955).
29. R. Flatt, *Forschung. Ingenieurwesen.* **51**(2):41 (1985).
30. R. Flatt, *Entropie* **149**:48 (1989).
31. R. Flatt and J. C. Trichet, *Euromech Colloquium 331 of Flows with Phase Transition*, Göttingen, 14–17 March (1995).
32. M. Vicentini-Missoni, J. M. H. Levelt Sengers, and M. S. Green, *J. Res. NBS* **73A**:563 (1969).
33. J. M. H. Levelt Sengers, W. L. Greer, and J. V. Sengers, *J. Phys. Chem. Ref. Data* **5**:1 (1976).
34. S. Angus, B. Armstrong, and K. M. de Reuck, *International Thermodynamic Tables of Fluid State. Carbon Dioxide* (Pergamon, Oxford, 1976).
35. J. Kestin, J. V. Sengers, B. Kamgar-Parsi, and J. M. H. Levelt Sengers, *J. Phys. Chem. Ref. Data* **13**:175 (1984).
36. J. V. Sengers et al., *Representative Equations for the Thermodynamic and Transport Properties of Fluids Near the G-L Critical Point, Final Report*, NASA Contractor Report 3424 (1981).
37. S. Tang and J. V. Sengers, *J. Supercrit. Fluids* **4**:209 (1991).
38. J. V. Sengers, in *Supercritical Fluids*, E. Kiran and J. M. H. Levelt Sengers, eds. (Kluwer Academic, Dordrecht, The Netherlands, 1994), p. 231.
39. G. X. Jin, S. Tang, and J. V. Sengers, *Int. J. Thermophysics* **13**:671 (1992).
40. A. van Pelt and J. V. Sengers, *J. Supercrit. Fluids* **8**:81 (1995).
41. E. A. Mason and T. H. Spurling, in *The International Encyclopedia of Physical Chemistry and Chemical Physics, Vol. 2. The Virial Equation of State*, J. S. Rowlinson, ed. (Pergamon, Elmsford, 1969).